euspen's 26th International Conference & Exhibition, Krakow, PL, June 2026

www.euspen.eu

Flexure-based inverted pendulum mechanical inclinometer

Loïc Tissot-Daguette[1], Salah Hasnaoui[1], Florent Cosandier[1], Charles Baur[1] and Simon Henein[1]

[1]Instant-Lab, EPFL, Switzerland

loic.tissot-daguette@epfl.ch

Abstract

This article presents a novel fully mechanical flexure-based single axis inclinometer with degressive sensitivity based on an inverted pendulum with visual readout. The mechanism comprises a cantilever beam with a tip mass attached to its free end inducing axial compression load in the beam, thus reducing its bending stiffness. By adjusting the mass, the sensitivity of the mechanism - defined as the ratio between the beam deflection and the inclinometer inclination - can be tailored. In theory, this sensitivity can approach infinity when the load exerted by the tip mass approaches the critical buckling load of the beam. However, increased sensitivity comes at the cost of reduced measurement range, increased nonlinearity and higher impact of manufacturing tolerances. An analytical model based on Euler-Bernoulli beam theory is developed to describe the degressive nonlinear relationship between beam deflection and inclination angle. The analytical model is validated through finite element modeling and experimental testing on a mesoscale titanium alloy prototype fabricated via wire electrical discharge machining. A graduated scale is integrated for direct visual readout of the deflection of the mass, enabling estimation of the inclination angle. Experimental results demonstrate that the designed inclinometer can be used to measure inclinations up to ±35°, with a sensitivity of 1.16 near the nominal position, degressively reducing to 0.425 near ±35°. The adjustable tip mass allows the sensitivity to be tuned for specific application requirements.

Inclinometer, Flexure mechanism, Stiffness reduction, Beam buckling, Degressive sensitivity

1. Introduction

In precision engineering, inclinometers (also called tilt sensors) are used to measure angular deviation relative to the direction of gravity. These devices are essential in a wide range of applications, including mechanical alignment and leveling [1], robotic motion control [2], and structural health monitoring [3].

Flexure-based inclinometers convert tilt angle into strain or displacement without friction and backlash, therefore offering accurate and repeatable measurements. However, their performance is often constrained by the limited deformation range of the compliant elements. Most existing designs consist of a vertical cantilever beam with a tip mass oriented downward in the nominal position [4-6]. In these pendulum-like configurations, the beam is subect to tensile loading, which increases the effective stiffness and consequently reduces both sensitivity and measurement range.

In contrast, the present study investigates an alternative inverted pendulum configuration where the cantilever beam is subjected to compressive loading, which reduces the beam's bending stiffness, thereby enhancing sensitivity to inclination. In Section 2, the mechanism is described, modeled using classical beam theory and simulated via Finite Element Method (FEM). Section 3 presents the experimental setup used to characterize the performances of a mesoscale inclinometer prototype. The results are presented in Section 4, followed by concluding remarks in Section 5.

2. Conceptual Design

2.1. Mechanism description

A schematic of the proposed inclinometer mechanism is shown in Fig. 1. The device consists of a cantilever beam with a weight (mass m) attached to its free end. When the base frame is inclined by angle α relative to the gravity vector, the gravitational force mg generates a moment onto the beam, causing its deflection. This results in a tip rotation angle β, which serves as the output signal corresponding to the applied inclination.

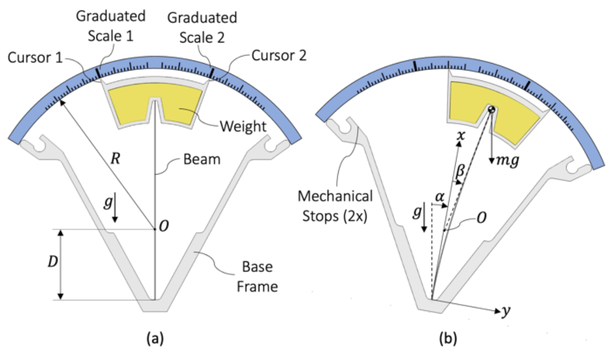

Figure 1. Schematics of the inclinometer (a) in neutral position (i.e., aligned with gravity orientation) and (b) inclined by an angle α

To measure β, one or more graduated scales can be affixed to the base frame. For instance, Fig. 1 illustatres two visual indicators (cursors) with respective graduated scales, that are labeled 1 and 2. This allows the inclination angle to be read from either the left or right side. These edges also act as reference points during the experimental characterization of the inclinometer (Sect. 3). For enhanced measurement accuracy, contactless displacement sensors (e.g., laser triangulation sensors) or strain-based sensing technologies (e.g., fiber Bragg gratings) could be integrated into the design to quantify the rotation angle β with higher precision than visual readout allows.

2.2. Analytical model

This section introduces the theoretical model used to design the inclinometer mechanism. For the calculations, we assume that the cantilever beam is initially straight, slender and aligned with the gravity vector (Fig. 1a). The beam, of length L, is clamped at one end and free at the other extremity. Figure 1b shows the deflection $y(x)$ and the load case of the beam when the base frame of the inclinometer is tilted. The center of mass of the weight is assumed to coincide with the free end of the beam. The gravitational force mg applied to the beam can be divided into a compressive axial force $F_x = mg\cos(\alpha)$ (along x) and a lateral force $F_y = mg\sin(\alpha)$ (along y). Considering small beam deformations, the beam deflection can be computed using Euler-Bernoulli beam theory:

$$M(x) = EIy''(x) \tag{1}$$

where, EI is the flexural rigidity and $M(x)$ is the bending moment. The general defection formula of a compressed beam with a fixed extremity at $x = 0$ is given by [7] as:

$$y(x) = A\sin(kx) + B(\cos(kx) - 1) + Cx \tag{2}$$

where $k = \sqrt{F_x/(EI)}$, and A, B and C are coefficients that are functions of the beam boundary conditions. Since $y'(0) = 0$ and $C = -F_y/F_x$ for small deformations [8], we have:

$$C = -Ak = -\tan(\alpha) \tag{3}$$

The bending moment being null at the beam free extremity (i.e., $M(L) = 0$), the combination of Eqs. (1) and (2) leads to the following relation:

$$B = -A\tan(kL) \tag{4}$$

The deflection angle $\beta = \arctan\big(y'(L)\big)$ can then be expressed as a function of the inclination angle α, as follows:

$$\beta(\alpha) = \arctan\big(\tan(\alpha)\,(\sec(kL) - 1)\big) \tag{5}$$

We define the inclinometer sensitivity at the vicinity of the nominal position as:

$$S_0 = \frac{d\beta}{d\alpha}(\alpha = 0) = \sec(k_0 L) - 1 \tag{6}$$

where $k_0 = \sqrt{mg/(EI)}$. It can be seen that the sensitivity S_0 can be tuned by adjusting the weight mass m. For instance, to obtain a sensitivity of $S_0 = 1$, the mass m must be selected such that $k_0 L = \pi/3$. If $k_0 L = \pi/2$, S_0 tends to infinity because the beam effective stiffness becomes null. Configurations close to this buckled state must be avoided because the measurement range is reduced and the function $\beta(\alpha)$ becomes highly nonlinear. For values of $k_0 L$ above $\pi/2$, the mechanism is bistable, leading to inclinometer reading that would suffer from hysteresis.

The graduated scales are considered to be circular with a radius R and a center O located at a distance D from the fixed extremity of the beam along the x-axis, see Fig. 1. The center O must coincide with the instantaneous rotation center of the beam free extremity in order for the trajectory of the cursors to follow their respective graduated scale. Hence, the relation $y_L = y(L) = (L - D)\tan(\beta)$ must be satisfied. Using Eqs. (2) to (5), the value of D can be expressed as:

$$D = L\left(1 - \frac{1}{kL}\frac{\tan(kL) - kL}{\sec(kL) - 1}\right) \tag{7}$$

2.3. Selected dimensions and materials

Using the analytical model in the previous section, a flexure-based mesoscale embodiment of the inclinometer is designed to demonstrate that the inclinometer works as expected, to provide numerical results for comparison to the analytical model and discuss possible manufacturing limits. The selected dimensions of the beam and the total mass of the weight are summarized in Table 1.

Table 1. Design parameters and corresponding values

	Parameter	Value
Cantilever beam	h	90 µm
	b	3 mm
	L	24.8 mm
Weight	m	4.085 g
Graduation	D	8.61 mm
	R	21 mm

The material of the flexure structure of the inclinometer is chosen to be titanium (Ti-Al6-V4). This material is well suited for its high yield strength (σ_y = 830 MPa) over Young's modulus (E = 114 GPa) ratio [9]. The main material of the weight is selected to be 18 karat gold, chosen for its high density. The total mass m = 4.085 g is the sum of the mass of the flexure structure at the free beam extremity and the mass of the gold weight.

The beam has a length L = 24.8 mm, a width b = 3 mm and a thickness h = 90 µm. Using Eq. (6), the nominal sensitivity is $S_0 = 1.16$. Equation (7) shows that D varies slightly with the inclination angle α. The value selected for D is chosen to correspond to the nominal position where $\alpha = 0$. Using the parameter values given in Table 1 and by substituting $kL = k_0 L$ in Eq. (7), this leads to $D \cong 0.347L$ = 8.61 mm.

The graduated scales (Fig. 1) are meant to be traced out using the formula $\beta(\alpha)$ given in Eq. (5) and considering a radius R = 21 mm. Note that due to the nonlinearity of $\beta(\alpha)$, the distance between two successive graduations is not constant.

Mechanical stops are integrated into the design to limit the rotation of the weight to within β = ±30°. Theoretically, this allows the measurement of inclination angles up to α = ±36°.

2.4. Finite element modeling

A finite element simulation was conducted using *COMSOL Multiphysics 6.1* to validate the analytical model described in Sect. 2.2. The inclinometer mechanism was modeled using the dimensions and material properties specified in Sect. 2.3. A stationary study was performed using the *Solid Mechanics* module to evaluate the structure's deformation under gravitational loading. Given the planar nature of the mechanism, the analysis was carried out in 2D under the *plane stress* assumption. *Geometric nonlinearity* was enabled, and a *segregated* approach was selected to accurately capture large deformations and potential buckling behavior.

The cantilever beam was discretized using mapped quadrilateral elements, with four elements across the thickness h and 200 along the length L. The remaining structure was meshed with free triangular elements.

A force of constant magnitude mg was applied to the free extremity of the cantilever beam while the base frame was fixed. The direction of the applied force was incrementally varied to simulate inclinations of the mechanism relative to gravity. Specifically, the inclination angle α was swept from -36° to 36° in 2° increments, where $\alpha = 0$ corresponds to the configuration where the force is compressive and aligned with the beam axis.

The tip rotation β, representing the inclinometer output, was extracted as a function of α, yielding the characteristic response $\beta(\alpha)$. The maximum of FEM von Mises stress in the structure was verified to be below the material yield strength. The FEM results are presented in Sect. 4.

3. Experimental method

The inclinometer structure is monolithically fabricated from titanium alloy using wire-cut electrical discharge machining (EDM). The gold weight is bonded on the moving block at the free beam end of the cantilever beam. The base frame of the flexure mechanism is rigidly mounted between two plexiglass plates.

The assembled inclinometer was installed on a precision rotary stage, with its rotation axis aligned with the center point O and oriented perpendicular to gravity. Inclination angles α were measured using a digital inclinometer (TESA Clinobevel 1-USB), offering a resolution of ±0.01°. A camera (Nikon D800 with AF-S NIKKOR 24-70mm f/2.8E ED lens) was used to measure the deflection angle β as a function of α. The direction of the camera was aligned with point O and its image plane coincided as much as possible with the inclinometer plane to minimize perspective distortion. The camera was placed at a distance of 0.8 m from the inclinometer.

Calibration was performed using a plumb bob, serving as an absolute vertical reference. The reference angle ($\alpha = 0$) was defined when the thread of the plumb bob, suspended between the inclinometer and the camera, was perpendicular to the line connecting two reference points M_1 and M_2 on the base frame.

Discrete inclination angles were applied by rotating the stage, with finer sampling near the nominal position. For each inclination angle, a photograph was captured while the mechanism was at static equilibrium. From each image, the reference frame (x, y) was reconstructed using the positions of M_1 and M_2. The deflection angle β was computed using the coordinates of points P_1 and P_2, based on their positions relative to point O. The final value of β for each inclination angle α was obtained by averaging the measured values from four independent measurement series.

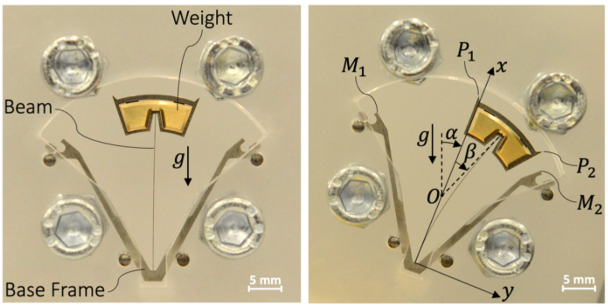

(a) (b)

Figure 2. Photographs of the inclinometer prototype (a) in neutral position and (b) inclined by an angle α

4. Results and discussion

Figure 3 shows the deflected angle β as a function of the inclination angle α, comparing the results from the analytical model, FEM simulation, and experimental measurements.

The FEM predicts similar results as compared with the analytical model, the relative error being bounded within 2.8%. In contrast, the experimental data labeled "before calibration" exhibit a noticeable offset from both models. The discrepancy cannot be explained by measurement uncertainty alone, as the maximum standard deviation in β is less than 0.54° (omitted from Fig. 3 for clarity).

When the inclinometer is aligned with gravity (i.e., at $\alpha = 0$), the deflection angle is $\beta_0 =$ -1.662°. This offset likely originates from manufacturing errors, such as geometric tolerances or residual stress, causing an initial beam deflection even in the absence of external load. Alternatively, it may result from a misalignment between the weight's center of mass and the x-axis in the nominal position.

To compensate for this systematic error, the inclinometer can be calibrated by rotating the graduated scale by the offset angle β_0 relative to the flexure structure. This ensures that $\beta = 0$ when $\alpha = 0$. The experimental data "after calibration" agree well with the analytical model, with a maximum relative error below 4.2%, confirming the accuracy of the theoretical formulation.

Given that the relationship $\beta(\alpha)$ is well predicted, the inclinometer is suitable for accurately determining inclination angles by reading the deflection β on integrated graduated scales (as shown in Fig. 1).

However, the experiments also revealed that the flexure-based mechanism exhibits a high quality factor (greater than 100) and a low eigenfrequency is (below 5 Hz). As a result, the inclinometer may require several minutes to settle after experiencing external vibrations. To improve damping and reduce stabilization time, it is suggested to immerse the flexure mechanism in a viscous fluid (e.g., water or glycerin), which would attenuate unwanted dynamic responses.

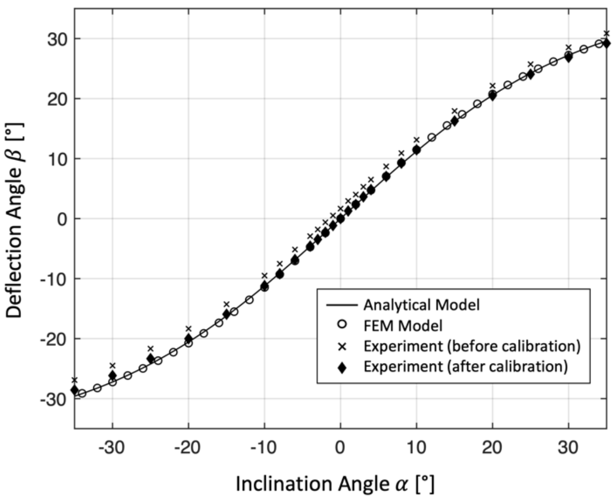

Figure 3. Graph of the deflection angle as a function of the applied inclination angle. The experiment data is plot before and after calibration, and is compared to the analytical and FEM models.

5. Conclusion

This paper presents a novel flexure-based inclinometer composed of a vertical cantilever beam and a tip mass. The mechanism functions as an inverted pendulum in its nominal position, deforming under gravitational load when tilted. The inclinometer exhibits maximum sensitivity of 1.16 near the nominal position (0°) and a minimal sensitivity of 0.425 at ±35°. This sensitivity decreases nonlinearly as the inclination increases. This degressive behavior offers the advantage of a higher measuring resolutions for small angles, while keeping a large measuring range. Analytical and FEM models have been developed to support the design process and predict the behavior of the mechanism. Experimental results agree closely with both models and confirm that the device can reliably measure inclination angles up to ±35°.

The continuation of this work will focus on sealing the mechanism within a viscous fluid (e.g., water or glycerin) to dampen unwanted oscillations and improve dynamic stability. Additionally, we plan to investigate the effect of increased tip mass to enhance sensitivity for applications requiring finer resolution.

Further prospect may include the extension of the measurement range to ±180° by using multiple cantilever beams oriented at different initial angles to provide continuous sensitivity over a full circle. Another avenue would be the extension of the flexure inverted pendulum principle to the design of a two-axis inclinometer by using a flexible rod (i.e., a beam with circular cross section) and a spherical visual readout grating.

References

[1] Chang H-Y, Chang Y-C and Liu W-F, 2017, A Highly Sensitive Two-Dimensional Inclinometer Based on Two Etched Chirped-Fiber-Grating Arrays, *Sensors*, **17**, 2922

[2] Besnard S and Khalil W, 1999, Calibration of parallel robots using two inclinometers, *Proceedings 1999 IEEE International Conference on Robotics and Automation*, **3**, 1758-1763

[3] Casas J R, Cruz P J, 2003, Fiber optic sensors for bridge monitoring, *Journal of Bridge Engineering*, **8(6)**, 362-373

[4] Pei H-F, Yin J-H and Jin W, 2013, Development of novel optical fiber sensors for measuring tilts and displacements of geotechnical structures, *Measurement Science and Technology*, **24**, 095202

[5] Yang Y, Ma X, Chen K, Wang E, Yu Z and Yu Q, 2018, A high-resolution dynamic fiber-optic inclinometer, *Sensors and Actuators A: Physical*, **283**, 305-312

[6] Zhang C, Zhang S and Cao J, 2023, In-place fiber-optic inclinometer based on a vertical cantilever beam and dual FBGs, *Optics & Laser Technology*, **159**, 108933

[7] Tissot-Daguette L, Smreczak M, Baur C and Henein S, 2021, Load cell with adjustable stiffness based on a preloaded T-shaped flexure pivot, *euspen's 21st International Conference & Exhibition, Copenhagen, DK*

[8] Tissot-Daguette L, Schneegans H, Thalmann E, Henein S 2022 Analytical modeling and experimental validation of rotationally actuated pinned–pinned and fixed–pinned buckled beam bistable mechanisms *Mech. Mach. Theory* **174** 104874

[9] Cosandier F, Henein S, Richard M, Rubbert L 2017 *The art of flexure mechanism design* EPFL Press Lausanne